Physica A 168 (1990) 260–267
North-Holland

FLUX CREEP AND VORTEX POTENTIAL WELL STRUCTURE IN HIGH-TEMPERATURE SUPERCONDUCTORS

Elia ZELDOV[1]
IBM Thomas J. Watson Research Center, Yorktown Heights, NY 10598-0218, USA

The resistive transition and the V–I characteristics in the presence of a magnetic field in epitaxial films of $YBa_2Cu_3O_7$, $Bi_2Sr_2CaCu_2O_8$, $YBa_2Cu_{2.985}Ag_{0.015}O_7$, and $GdBa_2Cu_3O_7$/$YBa_2Cu_3O_7$ multilayers have been investigated. The common qualitative features of all the systems are the current dependent thermally activated resistivity and the power law V–I characteristics at elevated current densities. An extended flux creep model, which incorporates the shape of the vortex potential well, is shown to account for these results.

1. Introduction

The mechanism of dissipation due to the flux motion in the mixed state of the high-temperature superconductors remains a controversial issue. While the thermally activated resistivity is consistent with the flux creep model [1], the power law voltage–current (V–I) characteristics have been ascribed, so far, either to the Kosterlitz–Thouless phase transition in the presence of low magnetic fields [2] or to the transition into the superconducting vortex-glass phase at elevated fields [3]. We present here a comprehensive study of the resistive transition and the V–I characteristics in various high-T_c systems in the presence of high magnetic fields. The essential qualitative features, i.e. thermally activated resistivity, nonlinear current dependence of the activation energy, and the power law V–I characteristics, are observed in all the systems, and hence must reflect an underlying *common* dissipation mechanism. The V–I characteristics in $Bi_2Sr_2CaCu_2O_8$ epitaxial films were found to be inconsistent with the vortex-glass picture as shown elsewhere [4]. We analyze the results within the framework of the flux creep model and show that the main features can be readily reproduced by incorporating the shape of the vortex potential well into the model [5].

[1] On leave from the Department of Electrical Engineering and Solid State Institute, Technion – Israel Institute of Technology, Haifa 32000, Israel.

2. Sample preparation

High-quality $YBa_2Cu_3O_7$, $Bi_2Sr_2CaCu_2O_8$, $YBa_2Cu_{2.985}Ag_{0.015}O_7$ and $GdBa_2Cu_3O_7/YBa_2Cu_3O_7$ epitaxial films were laser-ablated onto (100) $SrTiO_3$ substrates and patterned by an excimer-laser–microscope system to form microbridges typically 20 μm wide and 200 μm long [6]. The films were 0.4 to 0.6 μm thick and the multilayered $GbBa_2Cu_3O_7/YBa_2Cu_3O_7$ sample consisted of six periodic layers 200 Å each. The resistive data were obtained using the dc four-probe technique in the presence of a variable magnetic field of up to 6 T applied parallel to the c axis. Special care was taken to assure the absence of any heating effects in the relevant experimental regions.

3. Experimental results

Fig. 1 shows the resistive transitions in epitaxial films of different high-T_c materials at various magnetic fields and current densities. All the systems show two characteristic types of behavior, in the high and low resistivity regions. In the former region, ρ drops gradually with decreasing the temperature and the resistivity is current independent. These are the characteristics of the flux flow regime [7]. At lower temperatures, we observe the flux creep type of behavior in which the resistivity is thermally activated, $\rho = \rho_0 \exp(-U/kT)$, and the activation energy, U, is a complicated function of temperature, magnetic field, and current density and differs for various materials [4, 5, 8, 9]. The systems in fig. 1 represent different structures and various degrees of anisotropy; nonetheless, their resistive transition behavior is qualitatively very similar, indicating a common basic dissipation mechanism.

We investigate the behavior of the resistivity in the thermally activated region by analyzing the slopes of the curves in fig. 1, $U_{\mathrm{eff}} = -k\, \mathrm{d}(\ln \rho)/\mathrm{d}(1/T) = U - T\mathrm{d}U/\mathrm{d}T$, as shown in fig. 2a for the case of $YBa_2Cu_3O_7$. U_{eff} fits well the temperature dependence of the activation energy proposed by Tinkham [10]: $U(t) = U(0)\,(1 - t^2)(1 - t^4)^{1/2}$ where $t = T/T_c$. We want, however, to concentrate on the *current dependence* of U. In all the investigated systems, at elevated current densities, the activation energy is found to drop logarithmically with current [5, 8], as shown in fig. 2b. At low currents, on the other hand, the resistivity is current independent in the experimentally accessible temperature range. To complete the analysis, extensive measurements of the V–I characteristics were carried out in various systems in the presence of a magnetic field. Typical results are shown in fig. 3 in a more convenient form of the ρ–J characteristics. At elevated temperatures in the flux flow regime, the resistivity is current independent and decreases

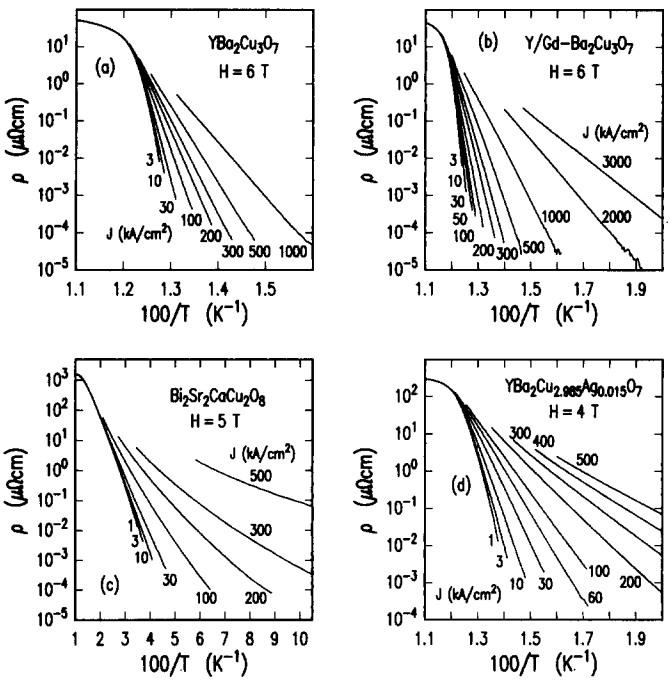

Fig. 1. Arrhenius plot of the resistivity of (a) $YBa_2Cu_3O_7$, (b) $GdBa_2Cu_3O_7/YBa_2Cu_3O_7$, (c) $Bi_2Sr_2CaCu_2O_8$, and (d) $YBa_2Cu_{2.985}Ag_{0.015}O_7$ epitaxial films at various current densities in presence of the indicated magnetic fields applied parallel to the c axis. At lower current densities the measured ρ is current independent.

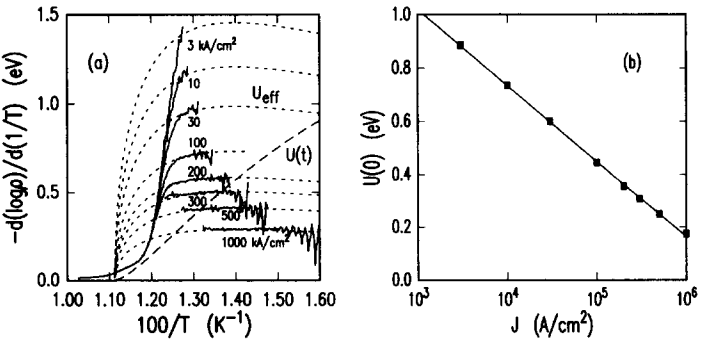

Fig. 2. (a) The logarithmic derivative of the resistivity of $YBa_2Cu_3O_7$ film in fig. 1a (solid lines), the theoretical activation energy $U(t) = U(0)\ (1-t^2)(1-t^4)^{1/2}$ (dashed), and the fit of the theoretical $U_{eff} = U(t) - t\mathrm{d}U(t)/\mathrm{d}t$ (dotted) to the experimental data. (b) The logarithmic current dependence of the activation energy as derived from (a).

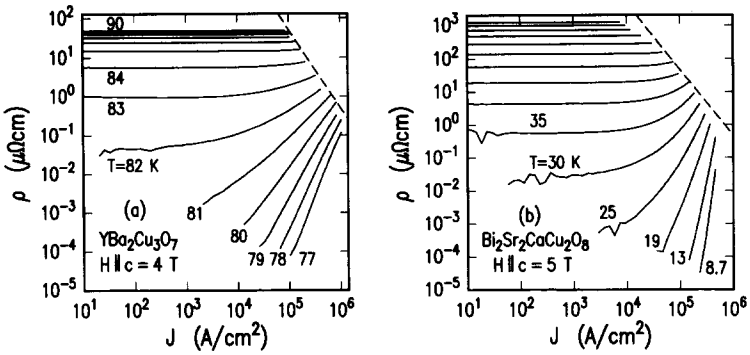

Fig. 3. The experimental $\rho-J$ characteristics of (a) $YBa_2Cu_3O_7$ and (b) $Bi_2Sr_2CaCu_2O_8$ films at various temperatures. The high-temperature curves are shown at 1 K (a) and 5 K (b) intervals. The dashed line in the upper-right corner is the limit of 1 mW power dissipation in the films, above which the measurements were limited by the self-heating effects.

gradually with cooling. At lower temperatures, where ρ drops below $\approx 10\%$ of ρ_n for $YBa_2Cu_3O_7$ and $\approx 2\%$ of ρ_n for $Bi_2Sr_2CaCu_2O_8$, we observe the flux creep behavior. Here the resistivity drops rapidly with decreasing T and shows a transition from current independent ρ at low currents to a nonlinear behavior at high-J values. The unique feature, observed in all the systems at elevated current densities, is the power law $\rho-J$ dependence.

4. Vortex potential well

We now discuss the results within the framework of the flux creep model [1]. At elevated temperatures the resistivity is determined by the flux flow viscous drag of the vortices, whereas at lower temperatures the dissipation mechanism is governed by the thermally assisted hopping of the flux lines or bundles, which are otherwise pinned due to some local defects. In the presence of a weak driving force, F, the net hopping rate is determined by the height of the potential barrier, regardless of the details of the potential well structure. At high F, however, the potential well is distorted and the resulting barrier height depends on the shape of the potential. Thus, the measurement of the relation between the driving force and the activation energy is a spectroscopic tool for the determination of the shape of the vortex potential well.

The potential structure that yields the experimentally observed logarithmic current dependence has a logarithmic conical shape [4, 5]. Fig. 4a shows schematically the potential, $V(x)$, which is a superposition of two logarithmical wells:

$$V(x)=\begin{cases} a\left[\ln\left(\dfrac{L-x}{L}\right)+\dfrac{x}{x_0}\right]-Fx\,, & 0\leq x\leq x_0\,,\\ a\left[\ln\left(\dfrac{x(L-x)}{x_0L}\right)+1\right]-Fx\,, & x_0<x<L-x_0\,,\\ a\left[\ln\left(\dfrac{x}{L}\right)+\dfrac{L-x}{x_0}\right]-Fx\,, & L-x_0\leq x\leq L\,, \end{cases} \tag{1}$$

where a and x_0 are the energy and the length scaling factors, L the distance between the neighboring wells, and the Lorentz driving force is $F = JBV_c$ with the flux bundle correlation volume, V_c. Such a potential well may arise due to a local defect that reduces the order parameter within a volume of a length scale of the coherence length, ξ. Since in these high-κ superconductors ($\kappa = \lambda/\xi$) ξ is very short, we expect a narrow conical structure of the well. On the other hand, since the penetration depth, λ, is large, the overlap between the defect and the logarithmically decaying magnetic field of a nearby vortex may contribute to the logarithmic broadening of the potential well through the diamagnetic energy term. We thus expect x_0 to be on the order of ξ, and the distance L between the wells to be the average distance between the defects in the case of an isolated vortex, or the Abrikosov flux lattice spacing, a_0, in the case of low defect density and flux bundle hopping.

The resistivity in the flux creep regime is determined by the net hopping rate in the direction of the driving force:

$$\rho=\frac{\nu_0 BL}{J}\left[\exp\left(-\frac{U^+}{kT}\right)-\exp\left(-\frac{U^-}{kT}\right)\right], \tag{2}$$

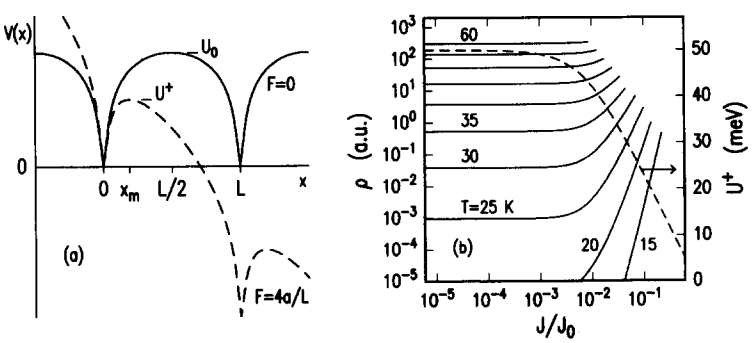

Fig. 4. (a) The shape of the logarithmic potential well of eq. (1) in absence (solid) and presence (dashed) of the driving force. (b) The theoretical $\rho-J$ characteristics (solid) from eqs. (2), (4) and (5) at various temperatures. The parameters of the logarithmic potential well, $U_0 = 50$ meV and $L/x_0 = 200$, were chosen to resemble the results in fig. 3b. The activation energy from eq. (5) (dashed) shows the logarithmic current dependence at high currents.

where U^+ and U^- are the barrier heights for hopping in the positive and negative direction, respectively, and ν_0 is the attempt frequency. At very low driving forces the potential is not distorted and we can apply the standard linear approximation [1] $U^{\pm} = U_0 \mp FL/2$ with $U_0 = a[\ln(L/4x_0) + 1]$, and the resulting current independent resistivity is

$$\rho = \frac{\nu_0 B^2 L^2 V_c}{kT} \exp\left(-\frac{U_0}{kT}\right). \tag{3}$$

A large driving force distorts the potential significantly, as shown schematically in fig. 4a, and the barrier location, x_m, becomes F-dependent,

$$x_m = \frac{L}{2}\left[\frac{F_0}{F} + 1 - \sqrt{\left(\frac{F_0}{F}\right)^2 + 1}\right], \qquad x_0 \leqslant x_m \leqslant \frac{L}{2}, \tag{4}$$

where $F_0 = 2a/L$. The corresponding barrier heights are

$$U^+ = a \ln\left(\frac{x_m(L - x_m)}{x_0 L}\right) + a - Fx_m, \qquad U^- = U^+ + FL. \tag{5}$$

For $F \ll F_0$ (and $FL < kT$), $x_m = L/2$ and the F-independent ρ of eq. (3) is reproduced. However, at $F \gg F_0$ (and $FL > kT$, $a > kT$) the linear approximation is not valid, $x_m = a/F$ and the activation energy obtains the *logarithmic* current dependence, $U^+ = a \ln(a/x_0 F) = a \ln(J_0/J)$, with the "critical" current $J_0 = a/x_0 B V_c$ at which U^+ drops to zero ($J < J_0$). The resulting ρ–J characteristics have a *power law* dependence rather than being exponential:

$$\rho = \frac{\nu_0 BL}{J}\left(\frac{x_0 F}{a}\right)^{a/kT} = \frac{\nu_0 BL}{J_0}\left(\frac{J}{J_0}\right)^{(a/kT)-1}. \tag{6}$$

Fig. 4b shows the theoretical ρ–J characteristics and the current dependence of the activation energy. The main features of the experimental results, namely the logarithmic $U(J)$ at elevated currents and the transition from current independent ρ to the power law behavior, are clearly presented in the theoretical plot. For an accurate fit to the experimental data one needs to take into account the temperature dependence of the potential structure, which was neglected in this simple analysis. In addition, the details of the curvature of the potential around $L/2$ will determine the broadening of the transition region in the ρ–J characteristics.

5. Conclusions

The power law V–I characteristics and the nonlinear current dependence of the activation energy appear to be a common feature of the high-T_c superconductors. We have shown that the conventional flux creep model may account for these results if the appropriate shape of the flux line potential well is incorporated into the theory. The logarithmic current dependence of the activation energy has significant practical, experimental and theoretical implications. In particular, the interpretation of the experimental data in the presence of high current densities, like in the critical current and magnetic relaxation measurements, has to be reevaluated in view of the above results.

Acknowledgements

The author is grateful to N.M. Amer, G. Koren, A. Gupta, M.W. McElfresh, R.J. Gambino and S.L. Shinde for fruitful collaboration and assistance at the various stages of the experimental work, to A.P. Malozemoff, Y. Yeshurun and M.P.A. Fisher for helpful discussions, and the US–Israel Educational Foundation for support.

References

[1] P.W. Anderson, Phys. Rev. Lett. 9 (1962) 309; P.W. Anderson and Y.B. Kim, Rev. Mod. Phys. 36 (1964) 39; M. Tinkham, Introduction to Superconductivity (McGraw-Hill, New York, 1975).

[2] M. Sugahara, M. Kojima, N. Yoshikawa, T. Akeyoshi and N. Haneji, Phys. Lett. A 125 (1987) 429; P.C.E. Stamp, L. Forro and C. Ayache, Phys. Rev. B 38 (1988) 2847; N.C. Yeh and C.C. Tsuei, Phys. Rev. B 39 (1989) 9708; T. Onogi, T. Ichiguchi and T. Aida, Solid State Commun. 69 (1989) 991; D.H. Kim, A.M. Goldman, J.H. Kang and R.T. Kampwirth, Phys. Rev. B 40 (1989) 8834.

[3] M.P.A. Fisher, Phys. Rev. Lett. 62 (1989) 1415; R.H. Koch, V. Foglietti, W.J. Gallagher, G. Koren, A. Gupta and M.P.A. Fisher, Phys. Rev. Lett. 63 (1989) 1511.

[4] E. Zeldov, N.M. Amer, G. Koren and A. Gupta, Appl. Phys. Lett. 56 (1990) 1700.

[5] E. Zeldov, N.M. Amer, G. Koren, A. Gupta, M.W. McElfresh and R.J. Gambino, Appl. Phys. Lett. 56 (1990) 680.

[6] A. Gupta, G. Koren, G.V. Chandrashekhar and A. Segmuller, Proc. SPIE Symp. Microelectronic Integrated Processing: High-T_c Superconductivity, Oct. 1989; G. Koren, A. Gupta, E.A. Giess, A. Segmuller and R.B. Laibowitz, Appl. Phys. Lett. 54 (1989) 1054; G. Koren, A. Gupta and R.J. Baseman, Appl. Phys. Lett. 54 (1989) 1920; S.L. Shinde and T.M. Shaw, Proc. First Int. Ceramic Science and Technology Congress, Anaheim CA, Oct. 31–Nov. 3 1989.

[7] A.P. Malozemoff, T.K. Worthington, E. Zeldov, N.C. Yeh, M.W. McElfresh and F.

Holtzberg, in: Strong Correlations and Superconductivity, H. Fukuyama, S. Maekawa and A.P. Malozemoff, eds., Springer Series in Solid State Sciences, vol. 89 (Springer, Heidelberg, 1989) p. 349.

[8] E. Zeldov, N.M. Amer, G. Koren, A. Gupta, R.J. Gambino and M.W. McElfresh, Phys. Rev. Lett. 62 (1989) 3093.

[9] T.T.M. Palstra, B. Batlogg, L.F. Schneemeyer and J.V. Waszczak, Phys. Rev. Lett. 61 (1988) 1662; T.T.M. Palstra, B. Batlogg, R.B. van Dover, L.F. Schneemeyer and J.V. Waszczak, Appl. Phys. Lett. 54 (1989) 763.

[10] M. Tinkham, Phys. Rev. Lett. 61 (1988) 1658.